Philosophical Magazine

ISSN: 1478-6435 (Print) 1478-6443 (Online) Journal homepage: http://www.tandfonline.com/loi/tphm20

Lattice distortion and charge density wave in $Na_2Ti_2Sb_2O$ revealed by scanning tunnelling microscopy

M. Q. Ren, Y. J. Yan, J. Jiang, S. Y. Tan, J. Miao, C. Chen, Y. Song, C. L. Zhang, P. C. Dai, B. P. Xie, T. Zhang & D. L. Feng

To cite this article: M. Q. Ren, Y. J. Yan, J. Jiang, S. Y. Tan, J. Miao, C. Chen, Y. Song, C. L. Zhang, P. C. Dai, B. P. Xie, T. Zhang & D. L. Feng (2017) Lattice distortion and charge density wave in $Na_2Ti_2Sb_2O$ revealed by scanning tunnelling microscopy, Philosophical Magazine, 97:7, 527-534, DOI: 10.1080/14786435.2016.1269217

To link to this article: http://dx.doi.org/10.1080/14786435.2016.1269217

Published online: 20 Dec 2016.

PHILOSOPHICAL MAGAZINE, 2017
VOL. 97, NO. 7, 527–534
http://dx.doi.org/10.1080/14786435.2016.1269217

Taylor & Francis
Taylor & Francis Group

Lattice distortion and charge density wave in $Na_2Ti_2Sb_2O$ revealed by scanning tunnelling microscopy

M. Q. Ren[a], Y. J. Yan[a], J. Jiang[a], S. Y. Tan[a], J. Miao[a], C. Chen[a], Y. Song[b], C. L. Zhang[b], P. C. Dai[b], B. P. Xie[a], T. Zhang[a,c] and D. L. Feng[a,c]

[a]State Key Laboratory of Surface Physics, Department of Physics and Advanced Materials Laboratory, Fudan University, Shanghai, China; [b]Department of Physics and Astronomy, Rice University, Houston, TX, USA; [c]Collaborative Innovation Center of Advanced Microstructures, Nanjing, China

ABSTRACT

$Na_2Ti_2Sb_2O$ is a parent compound of the titanium-based oxypnictide superconductors. It possesses a phase transition at T_s = 115 K whose nature is still unclear. Here we report a scanning tunnelling microscopy/spectroscopy (STM/STS) study on a $Na_2Ti_2Sb_2O$ single crystal. We observe a lattice distortion on the Na-terminated surface below T_s, which displays a 2 × 2 modulation (superstructure). The modulation vectors q = (±0.5, 0) $\frac{2\pi}{a}$ and (0, ±0.5) $\frac{2\pi}{a}$ match well with the Fermi surface nesting vectors observed by angle resolved photoemission spectroscopy (ARPES), and also agree with recent X-ray diffraction. A partially opened gap-like feature is present in STS near E_F. This evidences that the lattice distortion is driven by commensurate charge density wave order. Our results suggest the electron–phonon interaction is strong in $Na_2Ti_2Sb_2O$ and could be responsible for the superconductivity in titanium-based oxypnictides.

ARTICLE HISTORY
Received 1 July 2016
Accepted 1 December 2016

KEYWORDS
STM; experimental; crystal; $Na_2Ti_2Sb_2O$; charge density wave; lattice distortion

Introduction

Superconductivity occurs in many layered transition-metal compounds, such as cuprates [1], iron-based superconductors (IBS) [2] and transition-metal chalcogenides [3,4]. In these materials, the physics of the parent state or competing order such as charge/spin density wave (CDW/SDW) is essential for understanding the emergence of superconductivity. Recently, the titanium-based oxypnictides, namely (Ba, Na)Ti_2Pn_2O (Pn = As or Sb) have attracted much attention due to their layered structure and density wave-like instability [5–13]. In particular, with carrier doping, the density wave-like order in the parent compound is gradually suppressed and superconductivity emerges [7–10]. The phase diagrams of these materials also share strong similarity with cuprates and IBS [14,15]. For understanding the pairing mechanism in the Ti-based oxypnictides, identification of their parent state is of great importance. For example, unconventional superconductivity usually happens close to SDW (AFM) instabilities, while a CDW instability would lead to conventional s-wave superconductivity [6,16].

CONTACT D. L. Feng dlfeng@fudan.edu.cn

In the parent compounds of the Ti-based oxypnictides (i.e., $BaTi_2Pn_2O$ and $Na_2Ti_2Pn_2O$), a phase transition below a certain temperature T_s is universally observed [5–13], and much effort has been made to investigate its origin. Earlier theoretical works suggest the phase transition should arise from CDW/SDW due to strongly nested Fermi surface (FS) sections [6,16–19]. This scenario is supported by recent ARPES studies on $BaTi_2Sb_2O$ [12], $Na_2Ti_2Sb_2O$ [20] and $BaTi_2As_2O$ [21], and an STM study on $BaTi_2Sb_2O$ [12] which detected a CDW-like modulation. Meanwhile, nuclear magnetic resonance (NMR), neutron scattering and muon-spin relaxation studies on $BaTi_2Pn_2O$ did not find any magnetic structure, indicating that a SDW state may not exist [22–24]. Evidence for tetragonal symmetry breaking is observed in $BaTi_2Pn_2O$ from neutron diffraction [24] and nuclear quadrupole resonance [23] and in $Na_2Ti_2As_2O$ from Raman scattering [25], while powder neutron diffraction [26] and X-ray diffraction (XRD) [27] on $Na_2Ti_2Sb_2O$ reveal commensurate lattice distortions without any symmetry breaking. Besides CDW/SDW, other possibilities such as orbital ordering have also been proposed [24,28]. However, the parent state of Ti-based oxypnictides remains under debate and requires further investigation.

In this paper, we report a low temperature STM/STS study on high-quality $Na_2Ti_2Sb_2O$ single crystals with T_s = 115K. We observe a clear lattice distortion on the Na-terminated surface with a 2 × 2 superstructure. The corresponding modulation vector matches the nesting vector observed in ARPES. Moreover, a partially opened energy gap is detected in the dI/dV spectrum. Our results suggest that the lattice distortion may originate from a conventional and commensurate CDW order.

Experiment

High-quality $Na_2Ti_2Sb_2O$ single crystals were grown by a flux method as described in Ref. [20]. Temperature dependence of the resistivity and magnetic susceptibility were measured using Quantum Design PPMS. The STM experiments were performed in a low-temperature ultrahigh-vacuum STM system. Since $Na_2Ti_2Sb_2O$ degrades very quickly in air, we mounted the samples onto the sample holder in a glove box, and quickly transferred them to the STM chamber. The exposure time to air was limited to less than one minute. The samples were cleaved at about 77 K and immediately transferred into the STM module. Pt tips were used in all measurements after careful treatment on an Au (1 1 1) surface. STM topographic images were taken in constant current mode, and dI/dV spectra were collected using a standard lock-in technique with modulation frequency f = 975 Hz.

Results and discussion

The crystal structure of $Na_2Ti_2Sb_2O$ is composed of alternately stacked Ti_2Sb_2O layers and Na double-layers, as shown in Figure 1(a). The Ti_2Sb_2O layer shares some similarities with the CuO_2 layer in the cuprates and Fe_2As_2 layer in IBS. The resistivity and magnetic susceptibility measurements of our sample are shown in Figure 1(b). It is obvious that a sharp transition happens at ~115 K, characterised by a huge jump in the in-plane resistivity and a drop in the magnetic susceptibility, which is similar to previous reports [26,29–34]. Similar phase transitions are also observed in $Na_2Ti_2As_2O$ [29,30,33], $BaTi_2Pn_2O$ [7,21,22,35] and $R_2Ti_2Pn_2O$ (R = SrF, SmO) [36], indicating that they are universal to the parent compounds of the Ti-based oxypnictides [16,22–24,26–29].

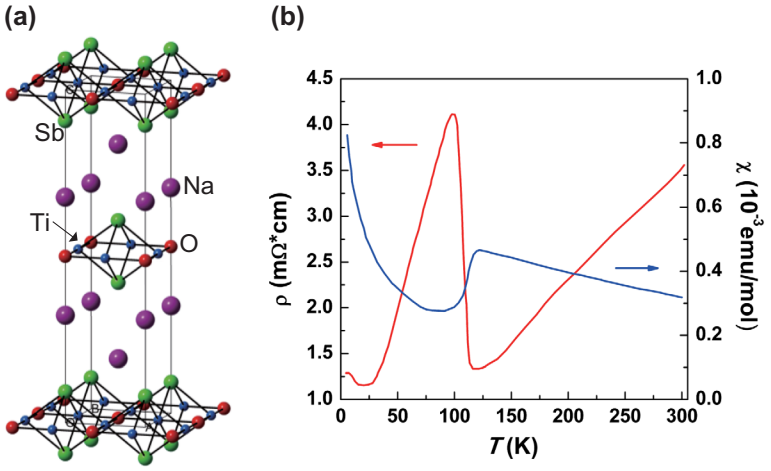

Figure 1. (colour online) (a) Crystal structure of $Na_2Ti_2Sb_2O$. Green, blue, purple, and red spheres represent Na, Ti, Sb and O atoms, respectively. (b) Temperature dependence of in-plane resistivity and magnetic susceptibility (H = 5T, H//ab) of $Na_2Ti_2Sb_2O$ single crystals.

The cleavage of $Na_2Ti_2Sb_2O$ happens between the double Na layers. Unlike $BaTi_2Sb_2O$, which cleaves in a single Ba layer resulting in a half covered, reconstructed Ba surface, the cleavage of $Na_2Ti_2Sb_2O$ is thought to leave an intact Na-terminated surface (similar to the case in $NaFe_{1-x}Co_xAs$ [37]). Figure 2(a) shows the typical image of a cleaved surface (taken at 4.5 K), which is atomically flat except some intrinsic defects. Figure 2(d) is a line-profile taken along the dashed line in Figure 2(a). One see that away from the defects, the surface corrugation is within few picometers; while around the defects the corrugation can exceed 40 pm, which could be due to defect-induced local states. An atomically resolved image of a defect free area is shown in Figure 2(b). It is noticeable that the surface lattice appears as distorted. As indicated by the green dots, the square unit cell of the original 1 × 1 lattice becomes rhombus like, resulting in a 2 × 2 superstructure (dashed square). The displacement of each Na atom, estimated from the line profiles of Figure 2(b) (as the one shown in Figure 2(e)), is about 5.8% of the 1 × 1 lattice constant. Figure 2(c) shows the fast Fourier transformation (FFT) of Figure 2(b). The Bragg spots corresponding to 1 × 1 lattice are marked as q_0, and the surface Brillouin zone of the undistorted lattice is illustrated by a dashed square. The modulation vectors at $q_1 = (\pm 0.5, 0)\,\frac{2\pi}{a}$ and $(0, \pm 0.5)\,\frac{2\pi}{a}$ correspond to the 2 × 2 superstructure. Spots at $q_2 = (\pm 0.5, \pm 0.5)\,\frac{2\pi}{a}$ appear as high-order harmonics of q_1, while they also coincide with possible FS nesting vectors as discussed later.

To further confirm the origin of the 2 × 2 superstructure, we performed dI/dV mappings which reflect the local density of states (DOS). The mappings are taken within a 40 nm × 40 nm area. In Figure 3(a)–(d), we show four representative maps taken at different bias energies. The 2 × 2 superstructure can be seen in all of these maps. The corresponding FFT images are shown in Figure 3(e)–(h). To avoid the influence of defect-induced local states, the regions near all the defect sites, as marked by dashed circles in Figure 3(a), are *excluded* before performing FFT. One can see that q_0–q_2 spots appear in all the FFT images. In Figure 3(i), we summarised the FFT line-cuts along the (0, 0)–(2π, 0) direction, taken at various energies and displayed in grey scale. Clearly, the q_0, q_1 are independent of energy, indicating they are from static orders. In Figure 3(j), we show two profile line-cuts of Figure

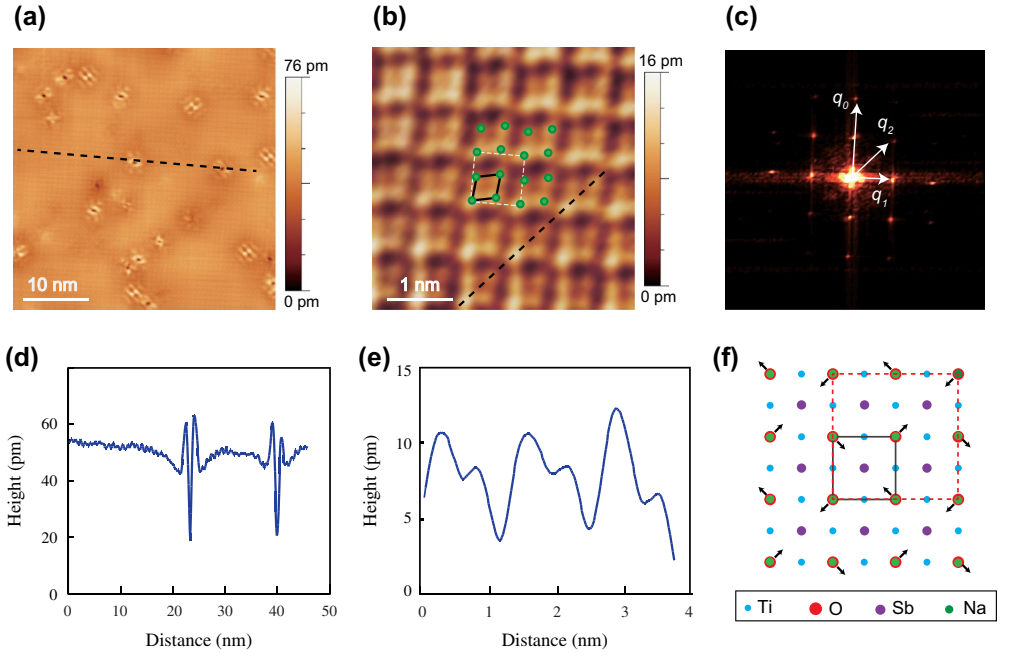

Figure 2. (colour online) (a) Typical topographic images of the Na terminated surface taken at 4.5 K ($V_b = -100$ mV, I = 100 pA). (b) Atomically resolved image taken at defect free area ($V_b = -15$ mV, I = 400 pA). The green dots represent the locations of Na atoms. The distorted lattice is indicated by the black rhombus. The dashed white square shows the unit cell of 2 × 2 superstructure. (c) FFT image of (b), scattering spots are marked by q_0–q_2. (d) Line cut profile taken along the dashed line in (a), shows the surface corrugation. (e) Line cut profile taken along the dashed line in (b), the displacement of Na atom can be seen. (f) The Na lattice distortion pattern predicted based on X-ray diffraction measurements for $Na_2Ti_2Sb_2O$ in Ref. [27].

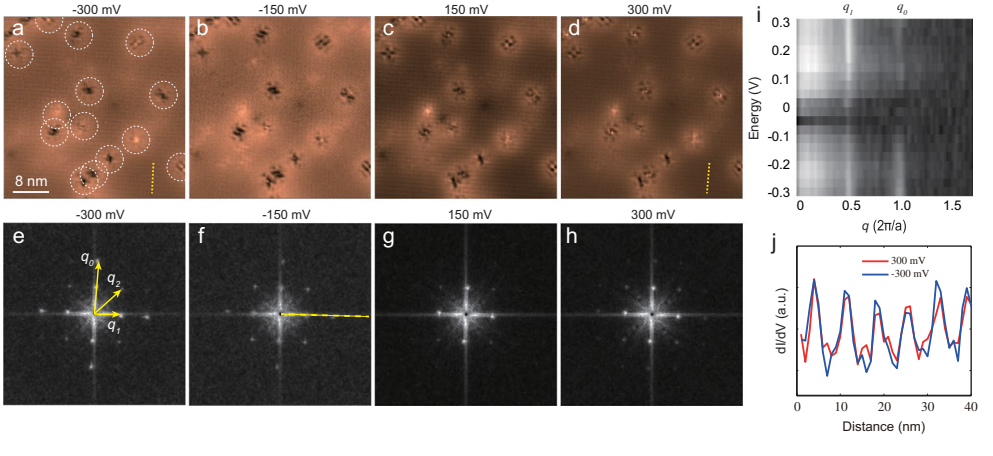

Figure 3. (colour online) dI/dV mapping on the Na-terminated surface of $Na_2Ti_2Sb_2O$ measured at 4.5 K. (a)–(d) Typical dI/dV maps of a 40 nm × 40 nm area taken at various energies. Each map has 300 × 300 pixels. (e)–(h) The corresponding FFTs of (a)–(d). Scattering spots are indicated by yellow arrows. (i) Line cuts extracted from the FFTs at various energies (along the dashed line in (f)), shown in grey scale. (j) Two line cuts taken along the dashed line in (a) and (d), respectively.

3(a) and (d), respectively. They are taken along the marked yellow dashed line at the exactly same location. One can clearly see the modulations from the 2 × 2 superstructure in both two line cuts, and particularly, they are spatially *in phase*. Since Figure 3(a) and (d) is taken at opposite energy (–300 and 300 mV), this further indicates the 2 × 2 superstructure is dominated by lattice distortion rather than electronic modulations [38].

Lattice distortion could be a signature of CDW transition, or may be from surface reconstruction, as which is observed in some cuprates and IBS materials [39,40]. However for $Na(Fe_{1-x}Co_x)As$, which also cleaves in between similar Na double layers, no surface lattice distortion is observed [37]. We noticed that a recent XRD study on $Na_2Ti_2Sb_2O$ did observe lattice distortion with the same modulation vectors as q_1 [27]. In their model, the Na layer follows the distortion of Ti_2Sb_2O layer. The displacement of each Na atom is shown in Figure 2(f). Clearly, the bulk unit cell is elongated along one diagonal and compressed along another, which matches the atomic structure we observe in Figure 2(b). A difference is that the relative displacement of Na atom observed here (5.8%) is much larger than the value extracted from XRD, which is only about 0.6% (0.025 Å). It could be due to that the measured surface is still different from the bulk. There may exist surface atom relaxations and modified surface phonon modes (although the interaction between the two Na layers are expected to be weak). However, the free surface should always reflect the symmetry breaking of the bulk. We note that in some materials such as $NbSe_2$ [41] and $NbSe_3$ [42] the surface even shows enhanced CDW temperature. Thus the matching of the surface distortion patterns with XRD would evidence the bulk lattice is distorted in a similar fashion.

CDW transition usually results from (partially) FS nesting in layered materials. In a previous ARPES study [20], the FS of $Na_2Ti_2Sb_2O$ has been mapped out. As sketched in Figure 4(a), the pockets at Γ, X and M do share some similarities in shape and size. In particular, the vector that connects X and M (also Γ and X) matches q_1, while the vector connecting Γ and M matches q_2. Both of these are present in Figure 2(c). This gives further evidence that the lattice distortion is from a CDW order driven by FS nesting. We point out that the measured FS of $BaTi_2Sb_2O$ [12] is similar to that of $Na_2Ti_2Sb_2O$; however, only the q_2 modulation is observed on $BaTi_2Sb_2O$ by STM [12]. We speculate that the strongly 2 × 1 reconstructed $BaTi_2Sb_2O$ surface hampers the detection of the underlying bulk lattice distortions, and the CDW phase in $Na_2Ti_2Sb_2O$ and $BaTi_2Sb_2O$ may actually be of similar origin.

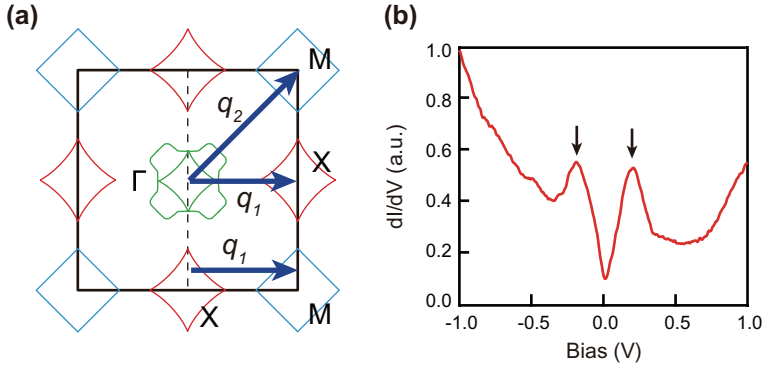

Figure 4. (colour online) (a) Schematic FS topology of $Na_2Ti_2Sb_2O$ measured by ARPES [20]. The arrows indicate possible FS nesting vectors. (b) Typical tunnelling spectrum of $Na_2Ti_2Sb_2O$ measured at 4.5 K with bias modulation amplitude of 10 mV.

In Figure 4(b), we show the dI/dV spectrum on the cleaved Na-terminated surface, which reflects the local DOS. The spectrum shows a clear gap-like feature with non-zero tunnelling conductance at gap bottom. The gap size determined by the two peaks (marked by arrows) is about ~200 meV, which is significantly larger than the gap reported by ARPES and optical measurement (~70 meV). We notice that a number of occupied bands of $Na_2Ti_2Sb_2O$, as observed by ARPES [20] have band top or bottom located in the energy range of –100 to –220 meV. Thus, it is possible to say that the DOS peak at –200 meV is contributed partially by the onset of such bands. However, since the gap feature is sharp and rather symmetric with respect to E_F, we speculate that it still evidences the reduced DOS at E_F, which is likely due to the CDW order. The rather large gap size (compare to T_s = 115K) could be an indication that the system is in the strong coupling regime [43].

To summarise, we clearly observe a lattice distortion on the cleaved surface of $Na_2Ti_2Sb_2O$. The agreement of the 2 × 2 modulation vector with the FS nesting vector, and the sharp gap-like feature in the DOS suggests the lattice distortion is from a commensurate bulk CDW state in $Na_2Ti_2Sb_2O$. The observed conventional CDW order suggests a phonon-mediated mechanism is likely responsible for the superconductivity in the $Na_2Ti_2Sb_2O$ system.

Disclosure statement

No potential conflict of interest was reported by the authors.

Funding

This work is supported by the National Science Foundation of China, National Key R&D Program of the MOST of China [grant number 2016YFA0300200]; National Basic Research Program of China (973 Program) [grant number 2015CB921700].

References

[1] J.G. Bednorz and K.A. Müller, *Possible high T_c superconductivity in the Ba–La–Cu–O system*, Z. Phys. B Condens. Matter 64 (1986), pp. 189–193.
[2] Y. Kamihara, T. Watanabe, M. Hirano, and H. Hosono, *Iron-based layered superconductor $La[O_{1-x}F_x]FeAs$ ($x = 0.05–0.12$) with $T_c = 26$ K*, J. Am. Chem. Soc. 130 (2008), pp. 3296–3297.
[3] S.Y. Li, G. Wu, X.H. Chen, and L. Taillefer, *Single-gap s-wave superconductivity near the charge-density-wave quantum critical point in $CuxTiSe_2$*, Phys. Rev. Lett. 99 (2007), p. 107001 (4p).
[4] W.Z. Hu, G. Li, J. Yan, H.H. Wen, G. Wu, X.H. Chen, and N.L. Wang, *Optical study of the charge-density-wave mechanism in 2H-TaS_2 and $NaxTaS_2$*, Phys. Rev. B 76 (2007), p. 045103 (5p).
[5] P. Doan, M. Gooch, Z.J. Tang, B. Lorenz, A. Möller, J. Tapp, P.C.W. Chu, and A.M. Guloy, *$Ba_{1-x}NaxTi_2Sb_2O$ ($0.0 \le x \le 0.33$): A layered titanium-based pnictide oxide superconductor*, J. Am. Chem. Soc. 134 (2012), pp. 16520–16523.
[6] D.J. Singh, *Electronic structure, disconnected Fermi surfaces and antiferromagnetism in the layered pnictide superconductor $NaxBa_{1-x}Ti_2Sb_2O$*, New J. Phys. 14 (2012), p. 123003 (11p).
[7] T. Yajima, K. Nakano, F. Takeiri, T. Ono, Y. Hosokoshi, Y. Matsushita, J. Hester, Y. Kobayashi, and H. Kageyama, *Superconductivity in $BaTi_2Sb_2O$ with a d^1 square lattice*, J. Phys. Soc. Jpn. 81 (2012), p. 103706 (4p).
[8] M. Gooch, P. Doan, B. Lorenz, Z.J. Tang, A.M. Guloy, and C.W. Chu, *High pressure study of the normal and superconducting states of the layered pnictide oxide $Ba_{1-x}NaxTi_2Sb_2O$ with $x = 0$, 0.10, and 0.15*, Supercond. Sci. Technol. 26 (2013), p. 125011 (5p).

[9] M. Gooch, P. Doan, Z.J. Tang, B. Lorenz, A.M. Guloy, and P.C.W. Chu, *Weak coupling BCS-like superconductivity in the pnictide oxide $Ba_{1-x}NaxTi_2Sb_2O$ (x = 0 and 0.15)*, Phys. Rev. B 88 (2013), p. 064510 (5p).

[10] H.F. Zhai, W.H. Jiao, Y.L. Sun, J.K. Bao, H. Jiang, X.J. Yang, Z.T. Tang, Q. Tao, X.F. Xu, Y.K. Li, C. Cao, J.H. Dai, Z.A. Xu, and G.H. Cao, *Superconductivity, charge- or spin-density wave, and metal–nonmetal transition in $BaTi_2(Sb_{1-x}Bix)_2O$*, Phys. Rev. B 87 (2013), p. 100502(R) (5p).

[11] U. Pachmayr and D. Johrendt, *Superconductivity in $Ba_{1-x}KxTi_2Sb_2O$ ($0 \le x \le 1$) controlled by the layer charge*, Solid State Sci. 28 (2014), pp. 31–34.

[12] Q. Song, Y.J. Yan, Z.R. Ye, M.Q. Ren, D.F. Xu, S.Y. Tan, X.H. Niu, B.P. Xie, T. Zhang, R. Peng, H.C. Xu, J. Jiang, and D.L. Feng, *Electronic structure of the titanium-based oxypnictide superconductor $Ba_{0.95}Na_{0.05}Ti_2Sb_2O$ and direct observation of its charge density wave order*, Phys. Rev. B 93 (2016), p. 024508 (9p).

[13] X.W. Yan and Z.Y. Lu, *Layered pnictide-oxide $Na_2Ti_2Pn_2O$ (Pn = As, Sb): A candidate for spin density waves*, J. Phys.: Condens. Matter 25 (2013), p. 365501 (9p).

[14] Ø. Fischer, M. Kugler, I. Maggio-Aprile, C. Berthod, and C. Renner, *Scanning tunneling spectroscopy of high-temperature superconductors*, Rev. Mod. Phys. 79 (2007), pp. 353–419.

[15] A. Martinelli, F. Bernardini, and S. Massidda, *The phase diagrams of iron-based superconductors: Theory and experiments*, C. R. Phys. 17 (2016), pp. 5–35.

[16] A. Subedi, *Electron-phonon superconductivity and charge density wave instability in the layered titanium-based pnictide $BaTi_2Sb_2O$*, Phys. Rev. B 87 (2013), p. 054506 (6p).

[17] F.F. Biani, P. Alemany, and E. Canadell, *Concerning the resistivity anomaly in the layered pnictide oxide $Na_2Ti_2Sb_2O$*, Inorg. Chem. 37 (1998), pp. 5807–5810.

[18] W.E. Pickett, *Electronic instability in inverse-K_2NiF_4-structure $Na_2Sb_2Ti_2O$*, Phys. Rev. B 58 (1998), pp. 4335–4340.

[19] D.V. Suetin and A.L. Ivanovskii, *Structural, electronic properties, and chemical bonding in quaternary layered titanium pnictide-oxides $Na_2Ti_2Pn_2O$ and $BaTi_2Pn_2O$ (Pn = As, Sb) from FLAPW–GGA calculations*, J. Alloys Compd. 564 (2013), pp. 117–124.

[20] S.Y. Tan, J. Jiang, Z.R. Ye, X.H. Niu, Y. Song, C.L. Zhang, P.C. Dai, B.P. Xie, X.C. Lai and D.L. Feng, *Photoemission study of the electronic structure and charge density waves of $Na_2Ti_2Sb_2O$*, Sci. Rep. 5 (2016), p. 9515 (6p).

[21] H.C. Xu, M. Xu, R. Peng, Y. Zhang, Q.Q. Ge, F. Qin, M. Xia, J.J. Ying, X.H. Chen, X.L. Yu, L.J. Zou, M. Arita, K. Shimada, M. Taniguchi, D.H. Lu, B.P. Xie and D.L. Feng, *Electronic structure of the $BaTi_2As_2O$ parent compound of the titanium-based oxypnictide superconductor*, Phys. Rev. B 89 (2014), p. 155108 (8p).

[22] Y. Nozaki, K. Nakano, T. Yajima, H. Kageyama, B. Frandsen, L. Liu, S. Cheung, T. Goko, Y.J. Uemura, T.S.J. Munsie, T. Medina, G.M. Luke, J. Munevar, D. Nishio-Hamane, and C.M. Brown, *Muon spin relaxation and electron/neutron diffraction studies of $BaTi_2(As_{1-x}Sbx)_2O$: Absence of static magnetism and superlattice reflections*, Phys. Rev. B 88 (2013), p. 214506 (5p).

[23] S. Kitagawa, K. Ishida, K. Nakano, T. Yajima, and H. Kageyama, *s-wave superconductivity in superconducting $BaTi_2Sb_2O$ revealed by $^{121/123}$Sb-NMR/nuclear quadrupole resonance measurements*, Phys. Rev. B 87 (2013), p. 060510(R) (5p).

[24] B.A. Frandsen, E.S. Bozin, H. Hu, Y. Zhu, Y. Nozaki, H. ageyama, Y.J. Uemura, W.-G. Yin and S.J.L. Billinge, *Intra-unit-cell nematic charge order in the titanium-oxypnictide family of superconductors*, Nat. Commun. 5 (2014), p. 5761 (7p).

[25] D. Chen, T.T. Zhang, Z.-D. Song, H. Li, W.-L. Zhang, T. Qian, J.-L. Luo, Y.-G. Shi, Z. Fang, P. Richard, H. Ding, *New phase transition in $Na_2Ti_2As_2O$ revealed by Raman scattering*, Phys. Rev. B 93 (2016), p. 140501 (5p).

[26] T.C. Ozawa, R. Pantoja, E.A. Axtell III, S.M. Kauzlarich, J.E. Greedan, M. Bieringer, and J.W. Richardson Jr, *Powder neutron diffraction studies of $Na_2Ti_2Sb_2O$ and its structure-property relationships*, J. Solid State Chem. 153 (2000), pp. 275–281.

[27] N.R. Davies, R.D. Johnson, A.J. Princep, L.A. Gannon, J.-Z. Ma, T. Qian, P. Richard, H. Li, M. Shi, H. Nowell, P.J. Baker, Y.G. Shi, H. Ding, J. Luo, Y.F. Guo, and A.T. Boothroyd, *Coupled commensurate charge density wave and lattice distortion in $Na_2Ti_2Pn_2O$(Pn = As, Sb) determined by X-ray diffraction and angle-resolved photoemission spectroscopy*, Phys. Rev. B 94 (2016), p. 104515 (9p).

[28] H. Nakaoka, Y. Yamakawa, and H. Kontani, *Theoretical prediction of nematic orbital-ordered state in the Ti oxypnictide superconductor $BaTi_2(As,Sb)_2O$*, preprint (2016). Available at arXiv,Phys. cond-mat.str-el/1511.08469.
[29] T.C. Ozawa and S.M. Kauzlarich, *Possible charge-density-wave/spin-density-wave in the layered pnictide-oxides: $Na_2Ti_2Pn_2O$ (Pn = As, Sb)*, Chem. Mater. 13 (2001), pp. 1804–1810.
[30] A. Adam and H.-U. Schuster, *Appearance and crystal structure of Pnictidoxide $Na_2Ti_2As_2O$ and $Na_2Ti_2Sb_2O$*, Z. Anorg. Allg. Chem. 584 (1990), pp. 150–158.
[31] E.A. Axtell III, T. Ozawa, and S.M. Kauzlarich, *Phase transition and spin-gap behavior in a layered tetragonal pnictide oxide*, J. Solid State Chem. 134 (1997), pp. 423–426.
[32] T.C. Ozawa and S.M. Kauzlarich, *Single crystal growth and characterization of a layered transition metal pnictide oxide: $Na_2Ti_2Sb_2O$*, J. Cryst. Growth 265 (2004), pp. 571–576.
[33] R.H. Liu, D. Tan, Y.A. Song, Q.J. Li, Y.J. Yan, J.J. Ying, Y.L. Xie, X.F. Wang and X. H. Chen, *Physical properties of the layered pnictide oxides $Na_2Ti_2P_2O$ (P = As,Sb)*, Phys. Rev. B 80 (2009), p. 144516 (5p).
[34] Y.G. Shi, H.P. Wang, X. Zhang, W.D. Wang, Y. Huang, and N.L. Wang, *Strong anisotropy in the electromagnetic properties of $Na_2Ti_2X_2O$ (X = As, Sb) crystals*, Phys. Rev. B 88 (2013), p. 144513 (5p).
[35] X.F. Wang, Y.J. Yan, J.J. Ying, Q.J. Li, M. Zhang, N. Xu, and X.H. Chen, *Structure and physical properties for a new layered pnictide-oxide: $BaTi_2As_2O$*, J. Phys.: Condens. Matter 22 (2010), p. 075702 (5p).
[36] R.H. Liu, Y.A. Song, Q.J. Li, J.J. Ying, Y.J. Yan, Y. He, and X.H. Chen, *Structure and physical properties of the layered pnictide-oxides: $(SrF)_2Ti_2Pn_2O$ (Pn = As, Sb) and $(SmO)_2Ti_2Sb_2O$*, Chem. Mater. 22 (2010), pp. 1503–1508.
[37] X. Zhou, P. Cai, A. Wang, W. Ruan, C. Ye, X. Chen, Y. You, Z.-Y. Weng, and Y. Wang, *Evolution from unconventional spin density wave to superconductivity and a pseudogaplike phase in $NaFe_{1-x}CoxAs$*, Phys. Rev. Lett. 109 (2012), p. 037002 (5p).
[38] J. Dai, E. Calleja, J. Alldredge, X. Zhu, L. Li, W. Lu, Y. Sun, T. Wolf, H. Berger and K. McElroy, *Microscopic evidence for strong periodic lattice distortion in two-dimensional charge-density wave systems*, Phys. Rev. B, 89 (2014), p. 165140 (5p).
[39] S.H. Pan, J.P. O'Neal, R.L. Badzey, C. Chamon, H. Ding, J.R. Engelbrecht, Z. Wang, H. Eisaki, S. Uchida, A.K. Gupta, K.-W. Ng, E.W. Hudson, K.M. Lang, and J.C. Davis, *Microscopic electronic inhomogeneity in the high-T_c superconductor $Bi_2Sr_2CaCu_2O_{8+x}$*, Nature 413 (2001), pp. 282–285.
[40] Y. Yin, M. Zech, T. Williams, X. Wang, G. Wu, X. Chen, and J. Hoffman, *Scanning Tunneling spectroscopy and vortex imaging in the iron pnictide superconductor $BaFe_{1.8}Co_{0.2}As_2$*, Phys. Rev. Lett. 102 (2009), p. 097002 (4p).
[41] B.M. Murphy, H. Requardt, J. Stettner, J. Serrano, M. Krisch, M. Muller, and W. Press, *Phonon modes at the 2H-$NbSe_2$ surface observed by grazing incidence inelastic X-ray scattering*, Phys. Rev. Lett. 95 (2005), p. 256104 (4p).
[42] C. Brun, Z.-Z. Wang, P. Monceau, and S. Brazovskii, *Surface charge density wave phase transition in $NbSe_3$*, Phys. Rev. Lett. 104 (2010), p. 256403 (4p).
[43] D.W. Shen, B.P. Xie, J.F. Zhao, L.X. Yang, L. Fang, J. Shi, R.H. He, D.H. Lu, H.H. Wen, and D.L. Feng, *Novel mechanism of a charge density wave in a transition metal dichalcogenide*, Phys. Rev. Lett, 99 (2007), p. 216404 (4p).